JETIR.ORG ISSN: 2349-5162 | ESTD Year : 2014 | Monthly Issue
JOURNAL OF EMERGING TECHNOLOGIES AND INNOVATIVE RESEARCH (JETIR)
An International Scholarly Open Access, Peer-reviewed, Refereed Journal

DEVELOPMENT AND PERFORMANCE EVALUATION OF AN ELECTRIC TRICYCLE WITH AN ADJUSTABLE WHEEL CAMBER

[1]Ikechukwu Celestine Ugwuoke, [2]Jamilu Shehu Musawa

[1,2]Department of Mechanical Engineering, Federal University of Technology, Minna, Nigeria.

Abstract : This research focused on the development and performance evaluation of an electric tricycle with an adjustable wheel camber. As efforts increase to improve the speed of tricycles used by the disabled through the use of electric motors, the need to investigate their stability as speed increases have become an important safety concern. Through the conscious choice of geometric parameters using steady-state cornering equations, the center of gravity location, tire cornering stiffness, and understeer gradient, a tricycle powered by an electric motor was developed having an adjustable wheel camber. Rollover analyses were carried out and a constant radius test was also carried out with different wheel camber angle adjustments of 0 degrees, 5 degrees, 10 degrees, and 15 degrees. Theoretical analyses and practical test results were compared. It was established that at 15m radius, even with a maximum camber angle of 15 degrees, the tricycle attained a maximum speed of 17km/h without the risk of tipping over. Wheel camber is seen to improve stability with a maximum speed of 11km/h attained at 0 degrees camber angle and 17km/h maximum speed attained at 15 degrees camber angle, all tested within a 15m radius turn.

IndexTerms **- Development, Performance evaluation, Stability, Tricycles, Geometric parameters, Understeer gradient, Wheel camber.**

I. INTRODUCTION

Tricycle is a popular means of transportation commonly seen in cities and rural areas in Nigeria. They are used to access public places like markets, schools, place of work, hospitals etc. These hand crank designs are limited in range and speed as they require much effort from the user and are also difficult to manoeuvre due to larger turning radius compared to the wheelchair. Due to mobility inconveniences, people with locomotive disabilities find it difficult to access public services such as health care, education, skills acquisition, labour market and other social services. According to a UNICEF report, 95% of children with disabilities in developing countries are out of school while 90% of them will never have access to education in their life time [1]. In Nigeria, there are an estimated 25 million people living with disabilities. In Kogi and Niger state alone, common disabilities involved mobility with about 32% and a half of the respondents (1093 respondents) in that research have no education, 20% had primary, 8% secondary and 2% tertiary, while a third of them are under 21 years of age and had no occupation [2].

To have a successful rehabilitation program an active life style must be encouraged. To achieve this, many variants of assistive devices for people with manipulative and locomotive disabilities, were developed. These devices enable them to perform many activities of daily life thereby improving their quality of life, maintain an increasingly independent life style and make them play a more productive role in society [3]. There is a wide body of research on mobility assistive devices globally. Though a report by United Nations Development Project UNDP shows that below 1% of the need for wheelchairs in Africa are being met through local production [4]. In addition, the sustainable development goals (SDG 11, target 11.2) stated that “By 2030, provide access to safe, affordable, accessible and sustainable transport systems for all, improving road safety, notably by expanding public transport, with special attention to the needs of those in vulnerable situations, women, children, persons with disabilities and older persons ”. Nigeria ratified the United Nations Convention on the Rights of People with Disabilities (CRPD) in 2007 and its optional protocol in 2010. In January 2019, the nation passed a disability rights bill which forms the basis for full social inclusion for the disabled. This will not be fully achieved except with the development of appropriate home grown technologies that will solve their mobility needs in public places like schools, work place, markets, and hospitals and even at home.

The disabled tricycle, like other three wheeled vehicles, will be associated with stability problems as speed increases. These types of tricycles are very narrow as they are designed to operate indoors and outdoors. This gives very little choice in terms of some of the important parameters that affect stability such as wheelbase and wheel track. As effort is made to increase their speed, it is important to design them for stability and also investigate the parameters that govern stability given their narrow configuration. The world health organization (WHO) mentioned that one of the risk factors related to the use of powered two and three wheel vehicles (PTW) is stability and among the key measures and interventions to increase PTW safety is vehicle configuration to enhance stability [5]. The aim of this work is to develop an electric tricycle for the disabled with enhanced speed and improved handling and lateral stability. The design will be used to evaluate the rollover speeds during lateral acceleration, during lateral acceleration in a turn, during braking in a turn. It will also be used to evaluate the understeer gradient and its effect on lateral acceleration response, velocity and curvature response. The effect of various degree of wheel camber angle against the stability of the tricycle will be studied.

II. MATERIALS AND METHOD

Materials used

Materials used in this work are:

1) Electric front drive hub motor 1000w, 48V
2) Controller 1000W, 48V
3) Speed LCD Display, 48V
4) Brake disc and caliper (2 quantity)
5) Throttle with reverse function
6) Brake lever (2 quantity)
7) Tires (3 quantity) 20 by 2.125, with load rating of 70 kg each, maximum pressure 60 psi
8) Lead acid Batteries (4 quantity), 12V, 7.2 AH
9) Linear String Encoder 24VDC, CALT CESI-S1000P for steering angle measurement;
10) Indicator, HB961 for readings of steering angle; 24VDC
11) Shock Absorber, DNM 165 (2 quantity)
12) 25mm stainless steel round tube
13) 30mm stainless steel round tube
14) 40mm stainless steel round tube
15) 20mm stainless steel square tube
16) Standard bicycle front fork

Materials used in this work were all sourced locally except the electric bicycle kit (consisting of items 1 to 6), the shock absorbers and the linear string encoder with display. Stainless steel was selected as the material for the frame because of strength and weight considerations. The batteries were selected due to availability instead of the lithium-ion battery commonly used with electric bicycle.

Design Consideration

The design considerations in this work were focused on achieving optimum level of stability within the performance parameters of the tricycle. Bicycle tire properties are insignificant at speed below 6m/s [6], however it was shown that bicycle tire properties, specifically cornering stiffness and camber stiffness, can influence handling and stability [7]. Other works show that light alternative vehicles stability and handling depends strongly on tire properties such as cornering stiffness and camber stiffness, though very little data is available on properties of bicycle and tricycle tires currently in the market [8]. The stability of the three wheeled vehicle, such as the tricycle, can be enhanced through thoughtful considerations of the centre of gravity (CG), wheelbase and wheel track [9]. The equations for the conditions for both handling stability and lateral stability are established through a bicycle model analysis. The major parameters that are significant to stability are the cornering stiffness, wheelbase, wheel track, CG location. The weight distribution and tire cornering stiffness affect the understeer gradient which is a major parameter for establishing vehicle stability. The understeer gradient will be improved by introducing camber angle to the rear wheels.

Handling Stability

The CG location is an important vehicle property. Proper location of the CG ensures the vehicle is stable in terms of reducing excess yaw response, reducing weaving at high speed, resist tipping over in turns and changes in road surfaces when sliding, swapping ends in braking due to weight transfer. Using established relationship between the neutral steer point (NSP), the static margin, tire cornering stiffness, steer angle, understeer gradient and steady state cornering equations, a conscious choice of geometric properties of the tricycle wheel be made to ensure the location of CG will enhance stability. The NSP is the point at which a side load can be applied and not cause a yaw response. The location of the NSP depends upon the total cornering stiffness C values at each end of the vehicle. The distance from the front axle line to the NSP is given by:

$$\text{LNSP} = \left[\frac{\bar{C}_R}{\bar{C}_F + \bar{C}_R}\right] \text{L} \quad (1)$$

Where,

C_F = cornering stiffness value of a single front tire (N/deg)

C_R = cornering stiffness value of a single rear tire (N/deg)

$\bar{C}_F$ = total cornering stiffness of the front tires (N/deg) = $2C_F$

$\bar{C}_R$ = total cornering stiffness of the rear tires (N/deg) = $2C_R$

L = wheel base

The character of the yaw response is determined by the location of the NSP relative to the CG. The distance from the CG rearward to the NSP divided by the wheelbase is termed static margin (SM), or as measured from the front axle line:

$$\text{SM} = \left[\frac{\bar{C}_R}{\bar{C}_F + \bar{C}_R} - \frac{l_1}{\text{L}}\right] \quad (2)$$

Where,

l_1 = distance from front axle line to CG, (m)

The value of SM can be positive, negative or zero and its value is an indicator of the yaw response of the vehicle. Consider a special case where the centre of mass is close to one half of the wheelbase from the front axle and the same types of tires are used at each end. In that case, $\bar{C}_F = \bar{C}_R$ and equation (2) can be rewritten as:

$$\text{SM} = \left[\frac{1}{2} - \frac{l_1}{\text{L}}\right] \quad (3)$$

From equation (3) above, it can be seen that when the centre of mass is at half the wheelbase, $l_1 = \frac{L}{2}$ then SM = 0. In this case a load at the *CG* will not produce a yaw response. The slip angle of the rear and front tires are equal and the vehicle will side slip. This condition is known as neutral steer (NS) and is considered stable. SM is positive (SM =+ve) when $\frac{l_1}{L}$ is less than one half of the wheelbase, when the CG is ahead of the NSP. The rear slip angle is less than the front slip and the vehicle heads up to the direction of the applied force. This condition is termed as under steer (US). When the *CG* is behind the NSP, then $\frac{l_1}{L}$ is larger than one half the wheelbase, the SM becomes negative (SM=-ve), where the rear slip angle is larger than the front and the vehicles heads against the direction of the applied force. This condition is known as over steer (OS) and is considered unstable. The above suggests that zero or positive values of SM are desirable for stability.

Vehicle response in a turn

During cornering, tires develop lateral force and also experience lateral slip. The application of Newton's second law along with the equations describing the geometry in turns is used to derive steady state cornering equations [10]. The lateral force, denoted by F_y is known as the cornering force.

$$F_y = C \propto \quad (4)$$

Where,
C = cornering stiffness
α = Slip angle

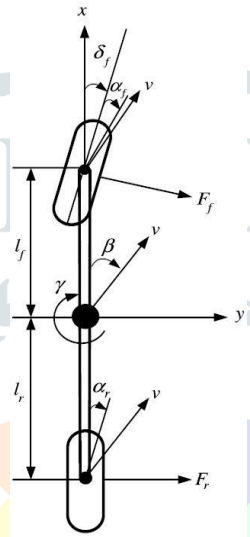

Fig. 1. Simplified steady state handling model for a two axle vehicle

Consider a vehicle travelling forward with a speed V, the sum of forces in the lateral direction at the tires must equal the mass times the centripetal acceleration.

$$\sum F_y = F_y f + F_y r = \frac{MV^2}{R} \quad (5)$$

Where,
F_{yf} = lateral cornering force at the front axle,
F_{yr} = lateral cornering force at the rear axle
M = vehicle mass
R = radius of turn
V = forward velocity

For moment equilibrium of the vehicle about its CG, the sum of the moment of the front and rear lateral forces must be zero.

$$F_{yf} b - F_{yr} c = 0 \quad (6)$$

$$F_{yf} = \frac{F_{yr} c}{b}$$

$$\frac{MV^2}{R} = F_{yr}\left(\frac{c}{b} + 1\right) = F_{yr}\left(\frac{b+c}{b}\right) = F_{yr}\left(\frac{L}{b}\right)$$

$$F_{yr} = \frac{Mb}{L}\left(\frac{V^2}{R}\right) \quad (7)$$

Mb/L is the portion of the mass carried by the rear axle i.e W_R/g. Equation 7 above implies that the lateral force developed at the rear axle is W_R/g times the lateral acceleration at that time. Solving for F_{yf} in a similar manner will show that W_F/g times the lateral acceleration at that time is the lateral force at the front axle. With the lateral forces known, the front and rear slip angles from equation (4) becomes,

$$\propto_F = W_F\left(\frac{V^2}{C_F g R}\right) \quad (8)$$

$$\propto_R = W_R\left(\frac{V^2}{C_R g R}\right) \quad (9)$$

From the geometry of Fig. 1 it was established that the steering angle δ becomes

$$\delta = 57.3\frac{L}{R} + (\propto_F - \propto_R) \quad (10)$$

Substituting equations (8) and (9) into equation (10), we get

$$\delta = 57.3\,\frac{L}{R} + \left[\frac{W_F}{C_F} - \frac{W_R}{C_R}\right]\frac{V^2}{gR} \quad (11)$$

The V^2/gR term is the lateral acceleration in terms of the fraction of g, and will be abbreviated as:

$$a_y = \frac{V^2}{gR} \quad (12)$$

Where,
V = velocity of CG along the path (m/s)
R = radius of the CG along the path (m)
g = acceleration due to gravity (m/s^2)

The term in bracket called the US gradient, and denoted with symbol *K* is important to this study.

$$K = \left[\frac{W_F}{\bar{C}_F} - \frac{W_R}{\bar{C}_R}\right] \quad (13)$$

Where:
W_F = weight on front wheels (N)
W_R = weight on rear wheels (N)

Substituting equations (12) and (13) into equation (11), we get

$$\delta = 57.3\frac{L}{R} + (K)(a_y) \quad (14)$$

The steering angle can also be expressed in terms of the static margin by combining equations (3) and (6) to yield:

$$\delta = 57.3\frac{L}{R} + (W)\left[\frac{\bar{C}_F - \bar{C}_R}{\bar{C}_F\bar{C}_R}\right](SM)(a_y) \quad (15)$$

To analyze stability in a turn, it is of interest to know how the steering angle δ changes as lateral acceleration a_y increases. Each expression for δ is the sum of a constant term, plus the expressions for $(\propto_F - \propto_R)$, K, and SM. The conditions that change the signs of these terms are equivalent: for example, when $\alpha_F > \alpha_R$, *then K>0 and SM>0*. What determines stability and defines the vehicles steer characteristics is the sign change of these terms.

Neutral steer: $\alpha_F = \alpha_R$, K=0, SM=0

Steering angle δ remains constant at the value 57.3 L/R, deg. If the vehicle was negotiating a circular path of radius R and slowly increasing the velocity, causing ay to increase, more lateral force would be needed at each end of the vehicle which would require slip angles αf and αr to increase. For a neutral steer vehicle, the vehicle centerline will slightly rotate relative to the direction of velocity V, decreasing the side slip angle β (which may become negative) and thus increase both front and rear slip angles the same amount as δ remains constant.

Understeer: $\alpha_F > \alpha_R$, K>0, SM>0

The needed steering angle increases with speed, as the front slip angle is larger than the rear. However, it is self-correcting. That is, if the driver does not increase δ, the positive yaw will turn the front of the vehicle toward the outside of the original path, thereby increasing the radius R and reducing the centrifugal force. Thus, a positive SM is termed stable.

Oversteer: $\alpha_R > \alpha_F$, K<0, SM<0

The needed steering angle is reduced from its neutral steer value, since the rear slip angle is larger than the front. That is, the rear is side slipping more than the front. If the driver makes no correction, the rear of the vehicle moves outward from the original path, decreasing the radius R and increasing the centrifugal force, requiring a greater correction. The correction is the familiar turn in the direction of the skid, and if done too late, one may not be able to catch the vehicle before it spins. Thus a negative SM is termed unstable.

Applications to three wheeled vehicle with a delta configuration

For delta tricycle configuration Equations 2 and 13 will be adjusted for the expressions of *SM* and *K* accordingly, but *K≥0 and SM≥0* condition for stability does not change. The expressions that must change are the cornering stiffness values. The cornering stiffness C_F value for the front wheel remain single while the rear tire will have its cornering stiffness value doubled denoted as $\bar{C}_R$ .The expressions for *K* and *SM* then becomes:

$$K = \left[\frac{W_F}{C_F} - \frac{W_R}{\bar{C}_R}\right] \quad (16)$$

$$SM = \left[\frac{\bar{C}_R}{C_F + \bar{C}_R} - \frac{l_1}{L}\right] \quad (17)$$

If the same tires are used on all three wheels and the weight distribution is equal on all the wheels then the threshold values of K=0 and SM=0 can be obtained. The tires will have the same cornering stiffness and the weight distribution will be:

$$W_F = \frac{W}{3} \quad (18)$$

$$W_R = \frac{2W}{3} \quad (19)$$

$$l_1 = \frac{2L}{3} \quad (20)$$

The cornering stiffness values in the expression for K are assumed to be constant for small slip angles for a given load. Since lateral force increases as ay increases, the relationship between lateral force versus slip angle moves beyond the linear range. There will be lateral weight transfer from the inside tires to the outside, however, due to load sensitivity the total cornering stiffness of the two rear tires would be less than the sum of their statically loaded values. The lateral weight transfer has significant design implications for a tricycle with delta configuration. The rear wheels will experience lateral load transfer consequently reducing the $\bar{C}_R$ value due to load sensitivity. From equation 16, it could be seen that this will produce a negative *K* value. To increase the value of $\bar{C}_R$ rear wheel camber will be introduced.

Wheel Camber Consideration to improve stability

Wheel camber has an influence on the lateral force generated at the contact patch known as camber thrust denoted as $F_y\gamma$ [11]. There is no available data for camber stiffness for the 20 by 2.125 bicycle tire. Four different camber angles, 0, 5, 10 and 15, will be used. Limiting the angle to 15 degrees is necessary since excessive camber angle promotes tire wear. The tricycle will incorporate a mechanism to vary the tire camber during testing.

Design Consideration for Rollover stability

A quasi static model is used to identify the level of lateral acceleration, a_y, that causes the inside tires to have zero vertical loads [12]. That level of lateral acceleration is called the rollover threshold. The value for a three wheeler involves the longitudinal placement of the CG as well as its height, and the vehicle track. The below equations were derived from the geometry of a three wheel vehicle with delta configuration while negotiating a turn.

$$\sum M_{TT} = -Wl_2\sin\theta + \frac{W}{2.22g}ah\cos\theta < 0 \quad (21)$$

The relationship can be re-written

$$\frac{a}{g} < \frac{l_2}{h}\tan\theta \quad (22)$$

Note that θ is a function of the geometry of the vehicle; thus it can be shown that:

$$\tan\theta = \frac{b}{2L} \quad (23)$$

Substituting equation (23) into (22) yields:

$$\frac{a}{g} < \frac{bl_1}{2hL} = F_c \quad (24)$$

Equation (24) is the condition required to prevent rollover. The lateral acceleration for a vehicle negotiating a curve of radius R can be expressed in terms of the forward speed V, and the turning radius as:

$$a = \frac{V^2}{R} \quad (25)$$

Substituting equation (25) into (24) yields equation for the speed at which rollover occurs.

$$V_{ro} = \sqrt{\frac{gRbl_1}{2hL}} \quad (26)$$

Rollover stability during lateral acceleration in a turn

Longitudinal acceleration will cause an inertia vector represented with symbol *A*. The lateral acceleration, resulting from the steady state turn, will cause an inertia vector represented by the symbol *E*. The symbol Z represents the resultant vector of *A* and *E*. The magnitude of the inertia force vectors A and E can be written as:

$$A = |\vec{A}| = \frac{W}{g}a \quad (27)$$

$$E = |\vec{E}| = \frac{W}{g}\frac{V^2}{R} \quad (28)$$

The resultant expression for the resultant inertia force vector $|\vec{Z}|$ is:

$$Z = |\vec{Z}| = \sqrt{A^2 + E^2 - 2AE\sin\gamma} \quad (29)$$

$$\emptyset = \tan^{-1}\left(\frac{E\sin\gamma - A}{E\cos\gamma}\right) \quad (30)$$

$$\theta = \tan^{-1}\left(\frac{b}{2L}\right) \quad (31)$$

The clockwise moment about the axis of tipping axis must be negative to ensure rollover stability while accelerating a turn. The rollover stability equation governing the three wheeled vehicle with a delta lay out is given as:

$$Z\cos\beta < \frac{Wbl_1}{2h\sqrt{L^2 + \left(\frac{b}{2}\right)^2}} \quad (32)$$

Where,

$$\beta = \emptyset + \theta$$

Rollover stability while braking in a turn

Symbol D represents the inertia force vector caused by braking. The magnitude of the vector can be written as:

$$D = |\vec{D}| = \frac{W}{g}d \quad (33)$$

The rollover stability equation when braking in a turn is given by:

$$Z\cos\beta < \frac{Wbl_1}{2h\sqrt{L^2 + \left(\frac{b}{2}\right)^2}} \quad (34)$$

Where,

$$\beta = \emptyset - \theta$$

To obtain the resultant vector Z and its orientation angle, ϕ, the inertia acceleration force A in equation (29) and (30) should be replaced with the negative of the inertia force, D, for braking in a turn.

Testing of Handling Characteristics: The Constant Radius Test.

The constant radius test will be used to determine the understeer gradient *K*. The experimental method is based on the equation:

$$\delta = 57.3\frac{L}{R} + K(a_y) \quad (35)$$

The Constant Radius Test involves driving in a circle of radius R at a steady speed and recording the steering angle, δ, and speed, V. Then incrementally increasing the speed and repeating the measurements until a specified maximum lateral acceleration, a_y, value is attained, or the vehicle is unable to maintain its path. The specified maximum lateral a_y value would be that which corresponds to the "tipping threshold". The speed reading will be taking form the speed display on the tricycle. A rotary string encoder will be used to measure the steering angle, δ, and the reading will be displayed on the indicator. The linear displacement

will be calibrated to correspond to angular displacement of the steering. The a_y value can be computed using equation (12). The understeer gradient K the tricycle can then be determined from the slope of the steer angle-lateral acceleration curve. From Equation (14), for a constant turning radius, the slope of the curve is given by

$$\frac{d\delta_f}{d\left(a_y/g\right)} = K \quad (36)$$

The K value obtained can be used to obtain motion variable of the tricycle such as yaw velocity response, lateral acceleration response, and curvature response, regarded as outputs to steering inputs from the driver.

Design calculations

The tricycle was developed with the geometric parameters tabulated in Table 1. The parameters were carefully considered in order to achieve optimum performance within its operational limitations.

Table 1. Geometric parameters

Parameter	Description	Value
L	Wheel base	1.2m
l_1	Length from CG to front axle	0.65m
l_2	Length from CG rearward to the rear axle	0.55m
b	Wheel track of vehicle	0.64m
W	Weight of vehicle and rider	120kg
h	Height of CG from the ground	0.55m
δ	Steering angle	3^0
R	Radius of turn	30m
V	Velocity	8.33m/s
g	Acceleration due to gravity	9.81m/s^2
a	Acceleration	6.5m/s^2
d	Deceleration	-5.27m/s^2

Calculation for rollover stability

Condition for rollover stability from equation (24) is given by

$$\frac{a_y}{g} < \frac{bl_1}{2hL}$$

Where,

$$a_y = \frac{V^2}{R} = \frac{8.33^2}{30} = 2.31\ {}^{m}/_{s^2}$$

Therefore,

$$\frac{2.31}{9.82} < \frac{0.64 \times 0.65}{2 \times 0.55 \times 1.20}$$

$$0.235 < 0.315$$

From the above solution, the condition for rollover stability was fulfilled.

Calculation for rollover velocity

The speed at which rollover occurs can be calculated from equation (26)

$$V_{ro} = \sqrt{\frac{gRbl_1}{2hL}} = \sqrt{\frac{9.82 \times 30 \times 0.64 \times 0.65}{2 \times 0.55 \times 1.2}} = 9.64 m/s\ (34.70 km/h)$$

From the above solution, rollover will occur at 34.70 km/h.

Calculation for rollover stability during lateral acceleration in a turn

The condition for rollover stability while accelerating in a turn is given in equation (32) as

$$Z\cos(\emptyset + \theta) < \frac{Wbl_1}{2h\sqrt{L^2 + \left(\frac{b}{2}\right)^2}}$$

Where,

$$\gamma = \delta = 3^o$$

$$A = |\vec{A}| = \frac{W}{g} \times a = \frac{120}{9.82} \times 6.5 = 79.43$$

$$E = |\vec{E}| = \frac{WV^2}{gR} = \frac{120 \times 8.33^2}{9.82 \times 30} = 28.26$$

$$Z = |\vec{Z}| = \sqrt{A^2 + E^2 - 2AE\sin\gamma} = \sqrt{79.43^2 + 28.26^2 - 2 \times 79.43 \times 28.26\sin 3} = 82.90$$

$$\emptyset = \tan^{-1}\left(\frac{E\sin\gamma - A}{E\cos\gamma}\right) = \tan^{-1}\left(\frac{28.26 \times \sin 3 - 79.43}{28.26 \times \cos 3}\right) = -2.76$$

$$\theta = \tan^{-1}\left(\frac{b}{2L}\right) = \tan^{-1}\left(\frac{0.64}{2 \times 1.2}\right) = 14.93$$

Therefore,

$$82.90 \times \cos(12.17) < \frac{120 \times 0.64 \times 0.65}{2 \times 0.55 \times \sqrt{1.20^2 + \left(\frac{0.64}{2}\right)^2}}$$

$$81.04 < 36.54$$

From the above solution, the condition for rollover stability during lateral acceleration in a turn was not fulfilled.

Calculation for rollover stability while braking in a turn

The condition for rollover stability while accelerating in a turn is given in equation (34) as

$$Z\cos(\emptyset - \theta) < \frac{Wbl_1}{2h\sqrt{L^2 + \left(\frac{b}{2}\right)^2}}$$

Where,

$$D = \left|\vec{D}\right| = \frac{W}{g} \times d = \frac{120}{9.82} \times (-5.27) = -64.40$$

$$E = \left|\vec{E}\right| = \frac{WV^2}{gR} = \frac{120 \times 8.33^2}{9.82 \times 30} = 28.26$$

$$Z = \left|\vec{Z}\right| = \sqrt{D^2 + E^2 - 2DE\sin\gamma} = \sqrt{-64.40^2 + 28.26^2 - 2 \times (-64.40) \times 28.26\sin 3} = 103.17$$

$$\emptyset = \tan^{-1}\left(\frac{E\sin\gamma - D}{E\cos\gamma}\right) = \tan^{-1}\left(\frac{28.26 \times \sin 3 + 97.76}{28.26 \times \cos 3}\right) = 3.52$$

$$\theta = \tan^{-1}\left(\frac{b}{2L}\right) = \tan^{-1}\left(\frac{0.64}{2 \times 1.2}\right) = 14.93$$

Therefore,

$$103.17 \times \cos(-11.41) < \frac{120 \times 0.64 \times 0.65}{2 \times 0.45 \times \sqrt{1.2^2 + \left(\frac{0.64}{2}\right)^2}}$$

$$101.13 < 36.54$$

From the above solution, the condition for rollover stability while braking in a turn was not fulfilled. The analytical calculations do not take into consideration the camber effect on the tricycle wheel.

Calculation for the determination of the centre of gravity

The tilting method was used for the CG height. The tricycle was placed parallel to the tilting axis (X). The wheels were supported. The tilting was done very slowly until the tricycle was no longer in a stable position and falls to the ground. The angle of the unstable position was measured. Three measurements were carried out independently and the average value of the three tilting angle was used for the calculation of CG's height. Tilting test was made on both directions determining two tilting angles: left side and right. The critical angle was established to be 30°. The CG height was calculated using the formula:

$$h = \frac{0.5 \times b}{\tan 30} = 0.55\text{m} \quad (37)$$

The CG's longitudinal location was established by measuring the front axle weight and the rear axle weight of the tricycle on a level surface.

$$\sum F_Y = 0$$

$$W - (R_f + R_r) = 0$$

$$W = (R_f + R_r) \quad (38)$$

$$\sum M_A = 0$$

$$R_f L - Wl_2 = 0 \quad (39)$$

$$l_2 = L\left({}^{R_f}/_{W}\right)$$

W_f=R_f and Wr=R_r

Wf =23.6Kg, Wr=26Kg

W=49.6Kg

$$l_2 = 1.2\left({}^{23.6 * 9.81}/_{49.6 * 9.81}\right) = 0.52\text{m}$$

The CG is located 0.52m from the rear of the tricycle with no rider on it. With a rider on the tricycle the front and rear weight distribution were measured as follows:

Wf =57.6Kg, Wr=68Kg

l_2 was calculated to be 0.55m.

There is a slight forward shift of the CG by 30cm

Calculation for weight distribution during acceleration

There is weight transfer from the front axle to the rear axle when accelerating on level ground. Here aerodynamic load is assumed to be zero.

$$W_F = W\left(\frac{l_2}{L} - \frac{ah}{gL}\right) = 125.60 \times \left(\frac{0.55}{1.2} - \frac{6.5 \times 0.55}{9.81 \times 1.2}\right) = 19.42\text{kg} \quad (40)$$

$$W_R = W\left(\frac{l_1}{L} + \frac{ah}{gL}\right) = 125.6\left(\frac{0.65}{1.2} + \frac{6.5}{9.81}\frac{0.55}{1.2}\right) = 106.18\text{kg} \quad (41)$$

Calculation for weight transfer when cornering

There is weight transfer from the inner to outer wheels when cornering. The rear wheels are affected for a three wheel vehicle with delta configuration.

$$W_{transfer} = \frac{W_r V^2 h}{gRb} = \frac{106.178 \times 8.33^2 \times 0.55}{9.81 \times 30 \times 0.64} = 21.51kg \quad (42)$$

III. FABRICATION

The fabrication of the tricycle involved simple processes like manual metal arc welding, bending, cutting, drilling, grinding, riveting and the use bolts and nuts. The fabrication was made in stages consisting of:

1) The rear carriage and rear axle assembly.
2) The main chassis
3) The front fork
4) The seat

The rear carriage consists of the rear axle, hub mount, rear wheels, hubs, brake caliper and disc, the shock absorber mounts. The rear carriage has an attachment point to the main chassis that carries a rubber bushing. Another attachment points were provided for shock absorbers. The hub mount is constructed to swivel and has a turnbuckle attached to it used for wheel camber adjustment. The main chassis was made from a 5cm stainless steel tube. The main tube was shaped by tube bending process and attached to a 3mm stainless steel angle section which formed the base for attaching the rear end. The steel tube for seat mounting was welded to the main tube. The mounting points for the battery compartment and the controller were welded to the main tube as well. The battery compartment was separately formed with a stainless steel flat bar. Disability leg rest mountings were welded to each end of the stainless steel angle section. The leg rest are detachable and gotten from a wheelchair. The front fork was removed from a road bicycle frame. It consists of the handle bar, the head tube, the speedometer, and brake levers. The electric wheel motor is mounted to the front fork. It is permanently welded to the main chassis. Additional foot rest were attached to the fork which can be used by people with normal leg function. Fig. 3 shows the tricycle foot rest.

Fig. 3. Tricycle foot rest

Fig. 4. Tricycle seat fabrication

The seat frame was constructed using a 1 inch stainless steel square tube. Standard bicycle seat springs were attached to provide comfort to the rider. Back rest was attached and adjustable side handles were riveted to the seat. The seat has a wooden base with foam glued to it and all covered with leather as shown in Fig. 4. The tricycle was painted with auto-based paint for a good finish and rust protection. The painting process involved washing to remove oil and dirt, application of body filler and putty to cover creases and kinks and smoothening with sand paper. Primer coat was applied for a thicker finish and then several layers of the cream colour paint applied. Dots of black spray were added for special effect. Fig. 5 shows the developed tricycle with adjustable wheel camber.

Fig. 5. Developed tricycle with adjustable wheel camber

IV. Results and Discussion

Analytical result

The condition for stability as indicated by equation 16 for K⩾0 is that the CG is located at L/3 from the rear axle to ensure that the tyres are carrying equal load. The CG position is treated as a design requirement to ensure that condition is met. Consequently, the CG is located 0.55m from the rear axle to ensure that the front tyre generates a higher cornering coefficient to achieve a positive Kus value. However, it can be seen that during acceleration there is significant transfer of weight from the front to the rear axle. This will generate higher normal loads on the rear tyres which will result to higher lateral loads and slip angles than the front tyre. This will likely affect the desired Kus value and consequently result to poor handling. The CG height was determined at 0.55m above the ground level from the experimental test. The figure was used in all the analysis. At a turn of 30m radius with a velocity of 8.33m/s the weight transfer when cornering, from the outer to the inner wheel is seen to be 21.51Kg. Furthermore, from the theoretical analysis of the rollover threshold it was established that:

1. From equation (24) the design has met the conditions for rollover stability
2. The rollover velocity from equation (26) was evaluated to be 34.70Km/h
3. From equation (32) the design failed to satisfy the conditions for rollover stability while accelerating in a turn
4. From equation (34) the design failed to satisfy the conditions for rollover stability while braking in a turn

The analytical calculations do not take into consideration the camber effect on the tricycle wheel. Table 2. Shows the comparison between theoretical and actual value of rollover velocity threshold for different radii at different wheel camber angles.

Table 2. Comparison between theoretical and actual value of rollover velocity threshold for different radii at different wheel camber angles.

Radius R(m)	*Theoretical* V_{ro} (Km/h)	*Actual at* 0^0 *Camber*	*Actual at* 5^0 *Camber*	*Actual at* 10^0 *Camber*	*Actual at* 15^0 *Camber*
5	14.15	6	8	9	9
10	20.00	9	12	13	14
15	24.52	11	14	15	17
20	28.30	14	15	18	19
25	31. 64	17	20	22	24
30	34.70				

Testing

From Table 2, it can be seen that wheel camber increases the rollover velocity threshold. There is significant difference between the actual and the calculated rollover velocity threshold. This could, in part, be attributed to the transient response of the tricycle during lateral acceleration. The speed threshold of 24km/h could not be exceeded during testing. For this reason, no rollover velocity was recorded for the 30m radius. All the camber angles at the 30m radius were tested at the maximum recorded speed of 24km/h with no corresponding risk of rollover. During testing of the tricycle a maximum speed of 27 km/h was reached on paved surface without cornering and tires inflated to 60psi. A constant radius test was carried out with 15m radius while adjusting the camber angle of wheel beginning at 0, 5, 10 and 15 degrees as maximum. The highest speed attained at 15m radius was 17Km/h, and the tricycle could not maintain its heading along the circular path. Fig. 3. Shows the constant radius test which requires the tricycle to attain a speed higher than the attained maximum of 27Km/h. As a result, the handling response could not be ascertained because the understeer gradient K was undetermined.

Fig. 3. Constant radius test.

Table 3. Values of speed, lateral acceleration and corresponding steering angle recorded

speed Km/h	lateral acceleration *ay* (g)	Steering angle δ			
		0^0 δ	5^0 δ	10^0 δ	15^0 δ
5	0.01332	5	5	5	5
10	0.05328	5	4	4	4
13	0.09004	2	3	3	3
16	0.13639				0
20	0.21311				
23	0.28185				
27	0.38840				

Table 3. shows the values of speed, lateral acceleration and corresponding steering angle recorded. During the test it can be seen that at 0 degrees camber, 15m radius the maximum speed reached before attempting to tip over is 11km/h. At 5 degrees camber only about 14 km/h was reached. At 10 degrees camber speed of 15km/h were reached while at 15 degrees camber speed of 17 km/h was reached. Above this speed there is high chance of tip over as the tricycle could not maintain its path. It is observed that wide gap exist between the theoretical and recorded velocities at which rollover occurs as shown in Table 2 and 3. This further support the analysis from equations (31) and (36) where the conditions for stability where not met with the geometric parameters used in the design. Due to scanty steering angle taken, the understeer gradient could not be ascertained. However, the effect of camber angle in improving lateral stability is very obvious. Fig. 6. Shows the wheel camber adjustment mechanism for the tricycle.

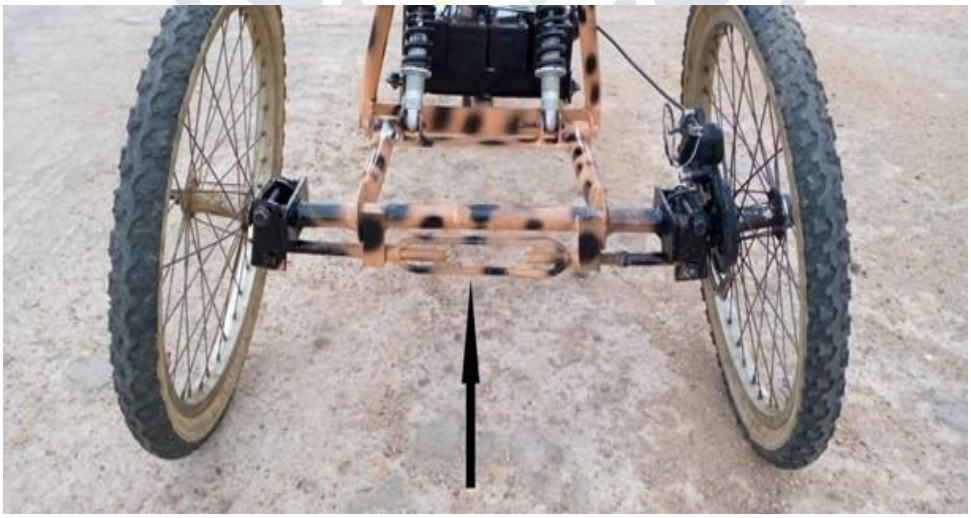

Fig. 6. Wheel camber adjustment mechanism.

As shown in Table 3, few readings were obtained for the steering angle due to limited speed and space. Only 15m radius full circle was obtainable. It can be seen that at 15m radius the maximum speed reached was 17km/h and the tricycle could no longer maintain the circular path. Higher speed records, beyond the maximum recorded speed of 27km/h, were required for the constant radius test. Consequently, the handling characteristic could not be ascertained since the understeer gradient, K, could not be determined. However, the result indicated that with low speed and significantly low levels of lateral acceleration the tricycle has tendency for oversteer characteristics and will have poor handling characteristics at higher speeds.

V. CONCLUSION

An electric tricycle with a variable wheel camber was developed intended for use by the disabled both indoors and outdoors. There is a wide variance between the calculated rollover velocity threshold and the actual as observed during field test. Data from practical tests will assist designers, manufacturers, regulators and users in making better decisions about the use of such powered tricycles. Wheel camber significantly improved the rollover stability of the tricycle. By cambering the wheel negatively, camber thrust acts opposite to the direction of the centrifugal force which creates a stabilizing effect. However, this effect also reduces the cornering coefficient which affects the understeer gradient, K, value, which may lead to poor steering response. Another reason for the improved rollover stability may be due to the slight increase in the wheel track by the negative camber. The results from the constant radius test could indicate poor handling characteristics at higher speeds as is common with most three wheeled vehicles. Specifically, tricycles handling are affected by the angle of the head tube. This research did not investigate the steering geometry as it affects handling of the tricycle. Stability and handling response are largely dependent on vehicle dimensions. Given the narrow dimensions, user safety is best achieved not only by designing stability into the tricycle. Some form of policy framework to serve as a regulation for manufacturers and users will be required. This may consider classification by the size, the user, use of technology etc and speed limitations for each class. Speed threshold can be selected for each class through a demonstrated ability to meet specified safety criteria. Data from practical tests like the one conducted in this work will help designers, manufacturers, regulators and users to make better decisions on the use of such powered tricycles. Disabled tricycles, both powered and manual, are usually operated within a shorter turn radius. The use of speed limiting devices and use of wheel camber and other means to enhance stability are highly required to enhance stability. Designs like this will help people with disability to live a more productive life style and improve their quality of life, to help the nation achieve its social inclusion policy and meet its sustainable development targets.

REFERENCES

[1] Factsheet: Inclusive and Basic Education For Children With Disabilities In Nigeria: The role of Federal and state Ministries of Education. Retrieved on January 15, 2019 from www.jonapwd.org
[2] Smith, N., (2011). The Face of Disability in Nigeria: A Disability Survey in Kogi and Niger States. Disability, CBR & Inclusive Development, 22(1), pp.35-47. DOI: http://doi.org/10.5463/dcid.v22i1.11
[3] Ebrahimi A, Kazemi AR, Ebrahimi A. (2016). Wheelchair Design and Its Influence on Physical Activity and Quality of Life Among Disabled Individuals. Iranian Rehabilitation Journal. 14(2):85-92. https://doi.org/10.18869/nrip.irj.14.2.8
[4] Winters, A., (2006). Wheelchair Design in Developing Countries. Accessed on January 5, 2019 from www.web.mit.edu/winter/public
[5] World Health Organisation (WHO)., 2017. Powered Two- & Three-Wheeler Safety: A Road Safety Manual For Decision-Makers And Practitioners. Accessed on 18 May, 2019 from www.who.int/publications/i/item/powered-two--and-threewheeler-safety
[6] Kooijman, J.D.G., Schwab, A.L., & Meijard, J.P., (2008). Experimental validation of a model of an uncontrolled bicycle. Multibody syst dyn 19, 115-132. https//doi.org/10.1007/s11044-007-9050-x
[7] Dressel, A., and Rahman, A., (2011). Measuring Sideslip and Camber Characteristics Of Bicycle Tyres, vehicle system dynamics, 50.8, 1365-1378, DOI: 10.1080/00423114.615408
[8] Windes, P., Archibald, M., (2013). Experimental Determination of Bicycle Tire Stiffness. ASEE North central conference 2013, Retrieved on May 16, 2019 From www.people.cst.cmich.ed
[9] Star, Patrick, J., Prof. (2006). Designing Stable Three Wheeled Vehicles, With Application to Solar Powered Racing Cars. Accessed February 8, 2019, from www.americansolarchallenge.org
[10] Gillespie, T.D., (1992). Fundamentals of Vehicle Dynamics. SAE International
[11] Wong, J.Y., (1993). Theory of ground Vehicles. New York, N.Y.: J. Wiley
[12] Huston, j., Graves, B., & Johnson, D. (1982). Three Wheeled Vehicle Dynamics. SAE Transactions, 91, 591-604. Retrieved May 27, 2019, from http://www.jstor.org/stable/44631967